Disorder-Driven Transition in the $\nu = 5/2$ Fractional Quantum Hall Effect

W. Zhu[1,2] and D. N. Sheng[3]

[1]*Institute of Natural Sciences, Westlake Institute of Advanced Study and School of Science, Westlake University, Hangzhou 030024, China*

[2]*Theoretical Division and CNLS, Los Alamos National Laboratory, Los Alamos, New Mexico 87545, USA*

[3]*Department of Physics and Astronomy, California State University, Northridge, California 91330, USA*

(Received 25 October 2018; revised manuscript received 9 May 2019; published 1 August 2019)

The fractional quantum Hall (FQH) effect at the filling number $\nu = 5/2$ is a primary candidate for non-Abelian topological order, while the fate of such a state in the presence of random disorder has not been resolved. We address this open question by implementing an unbiased diagnosis based on numerical exact diagonalization. We calculate the disorder averaged Hall conductance and the associated statistical distribution of the topological invariant Chern number, which unambiguously characterize the disorder-driven collapse of the FQH state. As the disorder strength increases towards a critical value, a continuous phase transition is detected based on the disorder configuration averaged wave function fidelity and the entanglement entropy. In the strong disorder regime, we identify a composite Fermi liquid phase with fluctuating Chern numbers, in striking contrast to the well-known $\nu = 1/3$ case where an Anderson insulator appears. Interestingly, the lowest Landau level projected a local density profile, the wave function overlap, and the entanglement entropy as a function of disorder strength simultaneously signal an intermediate phase, which may be relevant to the recent proposal of a particle-hole Pfaffian state or Pfaffian–anti-Pfaffian puddle state.

DOI: 10.1103/PhysRevLett.123.056804

Introduction.—The fractional quantum Hall (FQH) effect [1] is a novel example of topological orders [2], providing an ideal test bed for fractional statistics [3–6]. In particular, the quasiparticles obeying non-Abelian statistics are expected to form the building block for topological quantum computation [7,8] and thus is of crucial importance. Thus far, the even-denominator FQH system at the filling factor $\nu = 5/2$ is the most promising candidate for experimental realizations of non-Abelian states [9–17]. While this $\nu = 5/2$ state was first experimentally identified 30 years ago [9], its exact nature remains under intense theoretical debate. Among different candidates, the non-Abelian Pfaffian state [4] as a fully polarized $p_x - ip_y$ paired state of composite fermions [18] was numerically established as a viable possibility [19–26]. The Pfaffian state breaks particle-hole (PH) symmetry and has a partner state known as the anti-Pfaffian state [27,28], which is also a valid candidate. In the presence of an exact PH symmetry, for example by projecting into the first excited Landau level, the Pfaffian and anti-Pfaffian are exactly degenerate; thus the emergence of one over the other is determined by the PH symmetry breaking, e.g., through Landau level mixing [29–32]. However, very recently, the thermal Hall conductance of the $\nu = 5/2$ state is found to be $\kappa_{xy} \approx 5/2$ (in units of thermal conductance quanta) [33], inconsistent with the Pfaffian (anti-Pfaffian) state, for which thermal Hall conductance $\kappa_{xy} = 7/2(3/2)$ is expected.

The experimental observation of thermal Hall conductance $\kappa_{xy} = 5/2$ is intriguing and a challenge for theoretical understanding. One plausible interpretation is a PH symmetric Pfaffian (PH-Pfaffian) state realized at $\nu = 5/2$ [34–36], which is an s-wave pairing state built on Dirac composite fermions [37]. Thus far, existing numerical works [19–22,30–32] do not support the PH-Pfaffian state in microscopic models with dominant Coulomb interactions. One possible reason is that the PH-Pfaffian model wave function fails to represent a gapped and incompressible phase [38–40]. Moreover, the experimental observation can be alternatively explained by disorder-induced mesoscopic puddles made of Pfaffian and anti-Pfaffian states [41–44]. Compared to pure systems, there are limited studies of the role of random disorder on the 5/2 state, which immediately raises some critical questions: Is the PH-Pfaffian state or Pfaffian–anti-Pfaffian puddle state energetically favorable in a disordered FQH system? In light of the numerical supports of the Pfaffian (or anti-Pfaffian) in disorder-free systems, another important question is the following: What is the fate of the 5/2 FQH state in the presence of disorder? Generally, when the disorder strength becomes comparable to the strength of interactions between electrons, the FQH state will eventually be destroyed. A characterization of such a disorder-driven transition is highly desirable to compare with experimental observations [45]. To date, related studies of the disordered FQH systems have been done only at $\nu = 1/3$, where a disorder-driven transition from the Laughlin state to an Anderson insulator has been identified [46–48]. It remains unclear to what extent the above picture will change at $\nu = 5/2$.

In this Letter, we investigate the disorder-driven transition for the half-filled first excited Landau level, based on which we illustrate a global phase diagram for such a non-Abelian system in the presence of random disorder. First, we show that the distribution of Hall conductances and the associated topological invariant Chern number can be used to distinguish among different quantum phases. We identify a disorder-driven critical point separating the FQH state carrying a unique quantized Chern number, from a composite fermion liquid (CFL) that is characterized by a distribution of fluctuating Chern numbers for different disorder configurations. This is in sharp contrast to the $\nu = 1/3$ FQH state, where the Laughlin state undergoes a transition to an Anderson insulator [46,47] with a vanishing Chern number at the strong disorder side. This phase transition is also signaled by the variance of wave function fidelity and the disorder configuration averaged entanglement entropy, both of which support the same critical point for the collapsing of the FQH effect by strong disorder. In addition, we address the possibility of an intermediate phase in moderate disorder strength, potentially relevant to the disorder-induced PH-Pfaffian or Pfaffian–anti-Pfaffian puddle state. Our Letter not only identifies a novel quantum phase transition between the FQH state and a CFL but also provides strong evidence to support the theoretical conjecture of disorder-stabilized FQH phase based on numerical simulations of the microscopic model for FQH systems.

Model and method.—We consider N_e electrons moving on a torus under a perpendicular magnetic field. The torus is spanned by $\mathbf{L}_1 = L_1\mathbf{e}_x$ and $\mathbf{L}_2 = L_2\mathbf{e}_y$, where $\mathbf{e}_x$ and $\mathbf{e}_y$ are Cartesian unit vectors, and L_1 and L_2 are lengths of the two fundamental cycles of the torus. Required by the magnetic translational invariance, the number of fluxes penetrating a torus is equal to the number of orbitals in one Landau level $N_s = L_1L_2/(2\pi\ell^2)$ ($\ell = 1$ is the magnetic length). The total filling fraction is then defined as $\nu = \nu_0 + N_e/N_s$ ($\nu_0 = 2$ for 5/2 FQH systems due to the fully occupied lowest Landau level). When the magnetic field is strong, we can assume that electrons in the partially filled Landau level are spin polarized and their dynamics is restricted to the orbitals in the first excited Landau level. The many-body Hamiltonian is

$$\hat{H} = \sum_{m_i=0}^{N_s-1} V^{m_1,m_2}_{m_3,m_4}\hat{a}^\dagger_{m_1}\hat{a}^\dagger_{m_2}\hat{a}_{m_3}\hat{a}_{m_4} + \sum_{m_i=0}^{N_s-1} U^{m_1}_{m_2}\hat{a}^\dagger_{m_1}\hat{a}_{m_2},$$

where $a^\dagger_m(a_m)$ is the creation (annihilation) operator of an electron in the orbital m. By choosing Landau gauge, the momentum conserved interaction terms can be expressed as

$$V^{m_1,m_2}_{m_3,m_4} = \frac{1}{N_s}\delta^{\mathrm{mod}\,N_s}_{m_1+m_2,m_3+m_4} \times \sum_{q_1,q_2=-\infty}^{+\infty}\delta^{\mathrm{mod}\,N_s}_{q_2,m_1-m_4}V(\mathbf{q})e^{-(1/2)|\mathbf{q}|^2}e^{i(2\pi q_1/N_s)(m_1-m_3)},$$

where $V(\mathbf{q}) = 1/|\mathbf{q}|$ represents the Coulomb interaction and $\mathbf{q} = (q_x, q_y) = (2\pi q_1/L_1, 2\pi q_2/L_2)$. The disorder term is

$$U^{m_1}_{m_2} = \frac{1}{2\pi N_s}\sum_{q_1,q_2=-\infty}^{\infty}\delta^{\mathrm{mod}\,N_s}_{t,m_1-m_2}U(\mathbf{q})e^{-(1/4)|\mathbf{q}|^2}e^{i(\pi q_1/N_s)(2m_1-q_2)},$$

where $U(\mathbf{q}) = \int d\mathbf{r}e^{i\mathbf{q}\cdot\mathbf{r}}U(\mathbf{r})$ mimics the random disorder. To study the effects of correlated potential, we use the Gaussian correlated random potential $\langle U(\mathbf{q})U(\mathbf{q}')\rangle = (W^2/2\pi N_s)\delta_{\mathbf{q},\mathbf{q}'}e^{-2q^2\xi^2}$, where ξ is the correlation length.

We obtain the ground state $\{|\Phi_k\rangle\}$ of $\hat{H}$ using the exact diagonalization (ED) algorithm. Owing to the lack of translational symmetry in the presence of disorder, the system sizes accessible by ED are limited to $N_e \leq 12$ by the current computational capability. In our extensive tests, $N_e \leq 8$ systems suffer from very strong finite size effect, as the topological Pfaffian states are not fully developed for a pure system [22], so we will focus on $N_e = 10$, 12 below. We averaged up to 2000 and 500 samples for $N_e = 10$ and $N_e = 12$, respectively, which gives quantitatively reliable results.

Statistics of Chern number.—Identifying the topological invariant is crucial for characterizing the underlying physics of topological ordered states. Conventionally, FQH states are characterized by the Hall conductance and the associated Chern number [49–51], which determines the intrinsic topology of the wave function [52] and the corresponding gapless edge excitations at a system boundary [53]. In the presence of disorder, the Hall conductance also offers an unambiguous criterion to distinguish the insulating state from quantum Hall states in an interacting system [46,47,54]. To be specific, under twisted boundary conditions, the wave function becomes

$$|\Psi_k\rangle = \exp\left[-i\sum_{i=1}^{N_e}\left(\frac{\theta_1}{L_1}x_i + \frac{\theta_2}{L_2}y_i\right)\right]|\Phi_k\rangle,$$

where θ_i is the boundary phase and (x_i, y_i) is the coordinate of particles. The boundary phase averaged Hall conductance is $\sigma_H(k) = C_k e^2/h$, where C_k is defined as [46]

$$C_k = \frac{i}{4\pi}\oint_\Gamma d\theta\left(\left\langle\Psi_k\middle|\frac{\partial\Psi_k}{\partial\theta}\right\rangle - \left\langle\frac{\partial\Psi_k}{\partial\theta}\middle|\Psi_k\right\rangle\right).$$

Here, the closed path integral is carried out along the boundary Γ of the boundary parameter space (the magnetic Brillouin zone) $0 \leq \theta_1,\ \theta_2 \leq 2\pi$. C_k is equivalent to the

Berry phase (in units of 2π) accumulated when the boundary conditions evolve along the closed path Γ.

Let us start by discussing the salient features of the Chern number statistics for different disorder strengths. We tune the aspect ratio L_1/L_2 to find the energy spectrum with sixfold near degeneracy separated from other excited states, which characterizes the particle-hole symmetrized Pfaffian state [20]. Taking into account the fact that the lowest six states should become degenerate in the thermodynamic limit, we introduce probability $P(C)$ of the total Chern number distribution, which describes the probability that the total Chern number of the lowest $N_g = 6$ near degenerate states is C in our sample configurations. For a weak disorder strength [Fig. 1(a)], $P(C)$ takes unity for $C = 3$ and zero for $C \neq 3$ (i.e., the lowest six states have $C = 3$ for all the disorder configurations); thus each nearly degenerate ground state carries a Hall conductance of $\sigma_H = e^2/2h$, which manifests the $\nu = 5/2$ FQH state on a torus.

In the strong disorder regime, disorder tends to change the Chern number of each state and results in redistributions of probabilities of different Chern numbers. As shown in Fig. 1(a), when $W > 0.1$, $P(C)$ becomes nonzero for $C \neq 3$, with nearly equal probabilities for Chern numbers larger or smaller than 3 to appear in different disorder configurations. For example, at $W = 0.1$, $P(C = 3)$ is reduced to 0.95, while $P(C = 2) \approx 0.025$. Upon increasing disorder strength, $P(C = 3)$ monotonically decreases and the distribution of $P(C)$ becomes broader. The coexistence of different Chern numbers characterizes the delocalization of quasiparticle excitations. In particular, even though $P(C)$ has a broad distribution instead of a single nonzero value, we identify that the averaged Chern number remains approximately quantized to $\langle C \rangle \approx 3$, for example, $\langle C \rangle \approx 2.98$ at $W = 0.24$. This observation demonstrates that each ground state still carries nonzero averaged Hall conductance in the strong disorder regime, which is consistent with a CFL rather than an Anderson insulator [55]. Plausible understanding comes from the fact that various FQH $\nu = 5/2$ states, such as Pfaffian and anti-Pfaffian ones, can be interpreted as pairing states built on a half-filled CFL [37,66] with different underlying pairing symmetries [18]. While the transition follows the destruction of the pairing mechanism by disorder, disorder cannot localize composite fermions at half filling, since the backscattering and localization are suppressed due to the intrinsic π-Berry phase [67–71]. As a comparison, in the case of $\nu = 1/3$ FQH, strong disorder destroys the quantization of the Chern number and leads to $\langle C \rangle \approx 0$, which suggests a topologically trivial Anderson insulator in the disorder dominating regime [46,47,72].

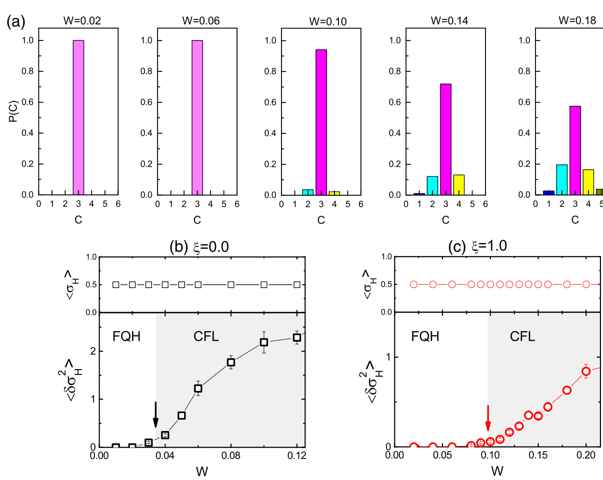

FIG. 1. (a) Probability distribution $P(C)$ of total Chern number C for various disorder strengths W. Here, we set $\xi = 1.0$ for a system with $N_e = 10$ electrons. The Hall conductance σ_H and its fluctuation $(\delta\sigma)_H^2$ versus disorder strength W for (b) $\xi = 0.0$ and (c) $\xi = 1.0$. The error bar shows the standard error in the disorder averaged value.

To quantify the evolution of Chern number statistics with respect to disorder strength, we demonstrate the fluctuation of the Hall conductance $\langle \delta\sigma_H^2 \rangle$ as a function of disorder strength W in Figs. 1(b) and 1(c). In the weak disorder regime, we observe that Hall conductance carried by each ground state is always quantized to $\langle \sigma_H \rangle = e^2/2h$ with little fluctuation $\langle \delta\sigma_H^2 \rangle \approx 0$. In the strong disorder regime, despite $\langle \sigma_H \rangle$ being quantized, the broad Chern number distribution leads to a finite fluctuation of the Hall conductance $\langle \delta\sigma_H^2 \rangle \neq 0$. We can identify a critical disorder strength W_c separating a FQH state with zero fluctuation from a critical state with finite fluctuations, as marked by arrows in Figs. 1(b) and 1(c). The above picture holds for all correlation lengths ξ and system sizes that we tested [56].

Entanglement entropy.—Topological phases are characterized by the long-range quantum entanglement patterns [73–75]. As a novel application, it is found that the entanglement entropy is sensitive to the quantum criticality in both clean systems [76,77] and disordered Abelian FQH systems [48,78]. Figure 2 shows the evolution of entropy by increasing disorder strength at $\nu = 5/2$ [79]. We find that the entropy S monotonically decreases with the increase of W. Importantly, a kink develops near the critical strength W_c [indicated by arrows in Fig. 2(a)], where the slope of entropy shows discontinuity [Fig. 2(b)].

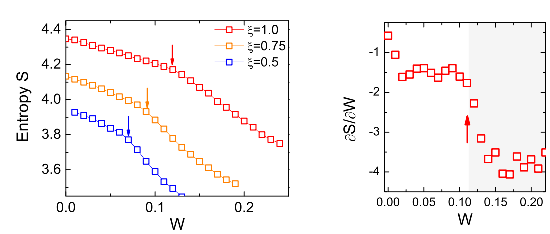

FIG. 2. (a) Entanglement entropy S versus disorder strength W of $N_e = 10$ electrons for various correlation lengths ξ. The data for different ξ are shifted in the vertical direction for clarity. (b) Derivative of entropy with respect to the disorder $\partial S/\partial W$ for $\xi = 1.0$.

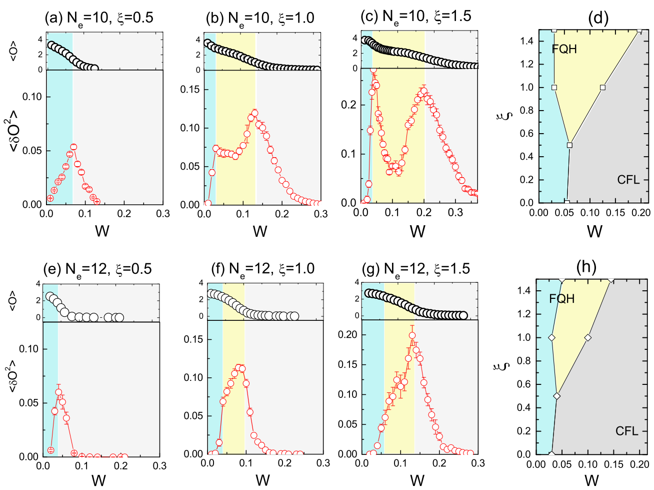

FIG. 3. Averaged wave function fidelity $\langle O\rangle$ and fluctuation of wave function fidelity $\langle \delta O^2\rangle$ as a function of disorder strength W for various correlation length $\xi = 0.5$, $\xi = 1.0$ and $\xi = 1.5$. The calculation is performed on the systems with $N_e = 10$ (top panel, a–c) and $N_e = 12$ (bottom panel, e–g). The intermediate phase is marked by light yellow which is determined by finite fluctuation $\langle \delta O^2\rangle$. The phase diagram determined from the $\langle \delta O^2\rangle$ is shown in (d) and (h).

This sudden change of $\partial S/\partial W$ shows a consistent signature of the expected quantum phase transition. Moreover, we also identify a trend of the increasing of the critical W_c for larger values of ξ. Importantly, the entanglement measurements give largely consistent identifications of the quantum critical point W_c compared to that identified by Chern number statistics (Fig. 1).

Implications for an intermediate phase.—The evolution of Hall conductance and its fluctuation unambiguously pin down the phase transition between the 5/2 FQH state and the CFL state. However, we are not able to distinguish the precise nature of different FQH states because possible candidates, including Pfaffian, anti-Pfaffian, or PH-Pfaffian states, carry the same Hall conductance. Next we further explore the phase transition at the wave function level. First, we define the wave function overlap matrix, $O_{ij} = \langle \Phi_i(W)|\Phi_j^{\mathrm{Pf}}(W=0)\rangle$, between the lowest six states for disordered system with the Pfaffian states, and the total overlap $\langle O\rangle$ (fidelity) as the summation of eigenvalues of the overlap matrix, where $\langle \cdots \rangle$ indicates the average over the disorder configurations. In Fig. 3, we show that the wave function fidelity monotonically decreases with the increase of the disorder, which does not show a clear signature of the possible quantum phase transition between different FQH states. Interestingly, we find that the fluctuation of wave function fidelity $\langle (\delta O)^2\rangle$ is sensitive to the phase transition. This is because, in the pure system, the wave function is characterized by a Pfaffian (anti-Pfaffian) wave function, which is a product of the Laughlin state for bosonic $\nu = 1/2$ and a $p_x \pm ip_y$ wave function for composite fermions. Physically, the fluctuation of wave function fidelity $\langle \delta O^2\rangle$ can detect the phase fluctuations of a wave function deviating from the $p_x \pm ip_y$ form. To be specific, we identify a single peak in $\langle \delta O^2\rangle$ for a short correlated length [Figs. 3(a) and 3(e)], which indicates a single phase transition by tuning disorder strength W. For disorder with a long correlated length, we find a two-step phase transition, evidenced by $\langle \delta O^2\rangle$ experiencing two sudden jump around W_* and W_c [e.g., Figs. 3(b) and 3(c)]. It demonstrates an intermediate regime with finite $\langle \delta O^2\rangle$ emerging between $W_* < W < W_c$. This observation signals an intermediate phase stabilized by correlated disorder. The upper bound of this intermediate regime W_c separates the FQH state from the non-FQH state, and the lower bound W_* indicates another transition point from a pure Pfaffian (or anti-Pfaffian) to an intermediate phase.

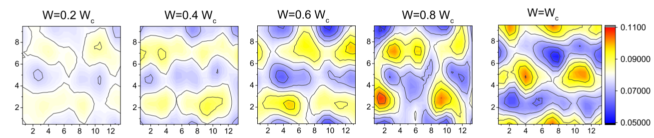

FIG. 4. The projected electron density $\rho(\mathbf{r})$ for various disorder strengths for $\xi = 1.0$ for systems with $N_e = 10$.

To inspect the effect of disorder in real space, we show the projected electron density $\rho(\mathbf{r})$ in Fig. 4, which is the equivalent electron density describing the spatial distribution of the guiding center [80–82]. The many-body density of states is qualitatively distinguishable from the pure limit: Density modulation is pronounced in spatial space and forms puddle structures starting from $W \gtrsim W_*$.

The appearance of additional critical strength W_* in the variance of wave function fidelity and projected electron density is suggestive of a possible intermediate phase stabilized by correlated disorder approximately within $W_* \lesssim W < W_c$. At the quantitative level, nonzero correlation length pushes the critical W_c to a larger value [Figs. 3(b), 3(c), 3(f), and 3(g)], leaving a wider region for the intermediate phase, which again indicates that an intermediate phase is favored by correlated disorder. Accordingly, we label an intermediate FQH phase in the phase diagram [Figs. 3(d) and 3(h)]. The intermediate regime exists on system sizes both $N_e = 10$ and $N_e = 12$, based on which we speculate that it would maintain in the thermodynamic limit. These observations are consistent with the theoretical pictures for the disorder stabilized PH-Pfaffian state [34] or Pfaffian–anti-Pfaffian puddle state [41–43].

Summary and discussion.—We have presented a systematic numerical study of correlated disorder-driven quantum phase transitions for the $\nu = 5/2$ fractional quantum Hall effect. First, the distribution of topological Chern numbers and corresponding Hall conductance fluctuations are capable of directly probing the collapse of the fractional quantum Hall state, which also determines the quantum critical points for random disorder with different correlation lengths. Second, the phase transition is also signaled by the wave function fidelity and entanglement entropy. The critical disorder strengths obtained from different methods are consistent with each other, validating the reliability of our numerical results. Third, in the strong disorder regime, we identify a composite Fermi liquid as the ground state, rather than an Anderson insulator as realized at filling number $\nu = 1/3$, demonstrating a rich physics for strongly correlated disorder systems. Last but not least, our results imply a possible intermediate phase stabilized by correlated disorder potentials, as evidenced by fluctuations of wave function fidelity and the puddlelike structures in projected densities of states. Although we cannot pin down the nature of the intermediate phase, these results provide the essential step towards understanding the nature of the disorder-stabilized $5/2$ quantum Hall state in the half-filled first excited Landau level from a microscopic point of view. We estimate that some existing experiments would fall into the intermediate regime (see Ref. [56]), which will motivate more experimental activities searching for the disorder-stabilized $5/2$ state. Furthermore, our work indeed opens up several directions for further exploration. For example, to connect with the previous studies on network models [41,42], it is important to identify the neutral chiral modes on the domain walls between randomly distributed puddles. In addition, the diagnosis of quantum fluctuations via various quantities shown here provides a practical way to study quantum criticality for general disordered, interacting fractionalized topological systems.

We thank F. D. M. Haldane, Bo Yang, Zhao Liu, Chong Wang, Yin-chen He, and Jie Wang for the stimulating discussions. W. Z. is partially supported by Westlake University and the U.S. Department of Energy (DOE), through the LDRD program at Los Alamos National Laboratory. D. N. S. is supported by the U.S. DOE, Office of Basic Energy Sciences, under Grant No. DE-FG02-06ER46305. D. N. S. also acknowledges the travel support from the Princeton MRSEC through National Science Foundation MRSEC Grant No. DMR-1420541.

[1] D. C. Tsui, H. L. Stormer, and A. C. Gossard, Phys. Rev. Lett. **48**, 1559 (1982).
[2] X. G. Wen, Int. J. Mod. Phys. B **04**, 239 (1990).
[3] R. B. Laughlin, Phys. Rev. Lett. **50**, 1395 (1983).
[4] G. Moore and N. Read, Nucl. Phys. **B360**, 362 (1991).
[5] M. Greiter, X. G. Wen, and F. Wilczek, Phys. Rev. Lett. **66**, 3205 (1991).
[6] N. Read and E. Rezayi, Phys. Rev. B **59**, 8084 (1999).
[7] A. Y. Kitaev, Ann. Phys. (Amsterdam) **303**, 2 (2003).
[8] C. Nayak, S. H. Simon, A. Stern, M. Freedman, and S. Das Sarma, Rev. Mod. Phys. **80**, 1083 (2008).
[9] R. Willett, J. P. Eisenstein, H. L. Störmer, D. C. Tsui, A. C. Gossard, and J. H. English, Phys. Rev. Lett. **59**, 1776 (1987).
[10] W. Pan, J.-S. Xia, V. Shvarts, D. E. Adams, H. L. Stormer, D. C. Tsui, L. N. Pfeiffer, K. W. Baldwin, and K. W. West, Phys. Rev. Lett. **83**, 3530 (1999).
[11] H. C. Choi, W. Kang, S. Das Sarma, L. N. Pfeiffer, and K. W. West, Phys. Rev. B **77**, 081301(R) (2008).
[12] W. Pan, J. S. Xia, H. L. Stormer, D. C. Tsui, C. Vicente, E. D. Adams, N. S. Sullivan, L. N. Pfeiffer, K. W. Baldwin, and K. W. West, Phys. Rev. B **77**, 075307 (2008).
[13] I. P. Radu, J. B. Miller, C. M. Marcus, M. A. Kastner, L. N. Pfeiffer, and K. W. West, Science **320**, 899 (2008).
[14] M. Dolev, M. Heiblum, V. Umansky, A. Stern, and D. Mahalu, Nature (London) **452**, 829 (2008).
[15] R. L. Willett, C. Nayak, K. Shtengel, L. N. Pfeiffer, and K. W. West, Phys. Rev. Lett. **111**, 186401 (2013).
[16] R. L. Willett, L. N. Pfeiffer, and K. W. West, Proc. Natl. Acad. Sci. U.S.A. **106**, 8853 (2009).
[17] Aveek Bid, N. Ofek, H. Inoue, M. Heiblum, C. L. Kane, V. Umansky, and D. Mahalu, Nature (London) **466**, 585 (2010).
[18] N. Read and D. Green, Phys. Rev. B **61**, 10267 (2000).
[19] R. H. Morf, Phys. Rev. Lett. **80**, 1505 (1998).
[20] E. H. Rezayi and F. D. M. Haldane, Phys. Rev. Lett. **84**, 4685 (2000).
[21] M. R. Peterson, K. Park, and S. Das Sarma, Phys. Rev. Lett. **101**, 156803 (2008).
[22] H. Wang, D. N. Sheng, and F. D. M. Haldane, Phys. Rev. B **80**, 241311(R) (2009).
[23] M. Storni, R. H. Morf, and S. Das Sarma, Phys. Rev. Lett. **104**, 076803 (2010).
[24] W. Zhu, Zhao Liu, F. D. M. Haldane, and D. N. Sheng, Phys. Rev. B **94**, 245147 (2016).
[25] A. E. Feiguin, E. Rezayi, C. Nayak, and S. Das Sarma, Phys. Rev. Lett. **100**, 166803 (2008).
[26] J. Zhao, D. N. Sheng, and F. D. M. Haldane, Phys. Rev. B **83**, 195135 (2011).
[27] M. Levin, B. I. Halperin, and B. Rosenow, Phys. Rev. Lett. **99**, 236806 (2007).
[28] S.-S. Lee, S. Ryu, C. Nayak, and M. P. A. Fisher, Phys. Rev. Lett. **99**, 236807 (2007).
[29] E. H. Rezayi and S. H. Simon, Phys. Rev. Lett. **106**, 116801 (2011).
[30] M. P. Zaletel, R. S. K. Mong, F. Pollmann, and E. H. Rezayi, Phys. Rev. B **91**, 045115 (2015).
[31] K. Pakrouski, M. R. Peterson, T. Jolicoeur, V. W. Scarola, C. Nayak, and M. Troyer, Phys. Rev. X **5**, 021004 (2015).
[32] E. H. Rezayi, Phys. Rev. Lett. **119**, 026801 (2017).
[33] M. Banerjee, M. Heiblum, V. Umansky, D. E. Feldman, Y. Oreg, and A. Stern, Nature (London) **559**, 205 (2018).
[34] P. T. Zucker and D. E. Feldman, Phys. Rev. Lett. **117**, 096802 (2016).
[35] J. Yang, arXiv:1701.03562.
[36] X. Chen, L. Fidkowski, and A. Vishwanath, Phys. Rev. B **89**, 165132 (2014).
[37] D. T. Son, Phys. Rev. X **5**, 031027 (2015).
[38] M. V. Milovanovic, Phys. Rev. B **95**, 235304 (2017).
[39] R. V. Mishmash, D. F. Mross, J. Alicea, and O. I. Motrunich, Phys. Rev. B **98**, 081107(R) (2018).
[40] A. C. Balram, M. Barkeshli, and M. S. Rudner, Phys. Rev. B **98**, 035127 (2018).

[41] D. F. Mross, Y. Oreg, A. Stern, G. Margalit, and M. Heiblum, Phys. Rev. Lett. **121**, 026801 (2018).
[42] C. Wang, A. Vishwanath, and B. I. Halperin, Phys. Rev. B **98**, 045112 (2018).
[43] B. Lian and J. Wang, Phys. Rev. B **97**, 165124 (2018).
[44] X. Wan and K. Yang, Phys. Rev. B **93**, 201303(R) (2016).
[45] N. Deng, G. C. Gardner, S. Mondal, E. Kleinbaum, M. J. Manfra, and G. A. Csáthy, Phys. Rev. Lett. **112**, 116804 (2014).
[46] D. N. Sheng, X. Wan, E. H. Rezayi, K. Yang, R. N. Bhatt, and F. D. M. Haldane, Phys. Rev. Lett. **90**, 256802 (2003).
[47] X. Wan, D. N. Sheng, E. H. Rezayi, K. Yang, R. N. Bhatt, and F. D. M. Haldane, Phys. Rev. B **72**, 075325 (2005).
[48] Z. Liu and R. N. Bhatt, Phys. Rev. Lett. **117**, 206801 (2016).
[49] D. J. Thouless, M. Kohmoto, M. P. Nightingale, and M. den Nijs, Phys. Rev. Lett. **49**, 405 (1982).
[50] Q. Niu, D. J. Thouless, and Y. S. Wu, Phys. Rev. B **31**, 3372 (1985).
[51] J. E. Avron, D. Osadchy, and R. Seiler, Phys. Today **56**, No. 8, 38 (2003).
[52] M. Kohmoto, Ann. Phys. (N.Y.) **160**, 343 (1985).
[53] Y. Hatsugai, Phys. Rev. Lett. **71**, 3697 (1993).
[54] D. P. Arovas, R. N. Bhatt, F. D. M. Haldane, P. B. Littlewood, and R. Rammal, Phys. Rev. Lett. **60**, 619 (1988).
[55] Further tests adding PH symmetry breaking three-body interactions confirm that the averaged Chern number remains unchanged even when PH symmetry is broken. Please see the Supplemental Material [56].
[56] See Supplemental Material at http://link.aps.org/supplemental/10.1103/PhysRevLett.123.056804, which includes Refs. [57–65], for additional results on statistics of Chern number and entanglement entropy, and the implications on existing experiments.
[57] S. M. Girvin, Phys. Rev. B **29**, 6012(R) (1984).
[58] Y. Huo, R. E. Hetzel, and R. N. Bhatt, Phys. Rev. Lett. **70**, 481 (1993).
[59] A. Y. Kitaev and J. Preskill, Phys. Rev. Lett. **96**, 110404 (2006).
[60] M. Levin and X. G. Wen, Phys. Rev. Lett. **96**, 110405 (2006).
[61] W. Pan, N. Masuhara, N. S. Sullivan, K. W. Baldwin, K. W. West, L. N. Pfeiffer, and D. C. Tsui, Phys. Rev. Lett. **106**, 206806 (2011).
[62] G. Gamez and K. Muraki, Phys. Rev. B **88**, 075308 (2013).
[63] J. P. Eisenstein, K. B. Cooper, L. N. Pfeiffer, and K. W. West, Phys. Rev. Lett. **88**, 076801 (2002).
[64] J. Nuebler, V. Umansky, R. Morf, M. Heiblum, K. von Klitzing, and J. Smet, Phys. Rev. B **81**, 035316 (2010).
[65] A. Kumar, G. A. Csáthy, M. J. Manfra, L. N. Pfeiffer, and K. W. West, Phys. Rev. Lett. **105**, 246808 (2010).
[66] B. I. Halperin, P. A. Lee, and N. Read, Phys. Rev. B **47**, 7312 (1993).
[67] S. D. Geraedts, M. P. Zaletel, R. S. K. Mong, M. A. Metlitski, A. Vishwanath, and O. I. Motrunich, Science **352**, 197 (2016).
[68] S. D. Geraedts, J. Wang, E. H. Rezayi, and F. D. M. Haldane, Phys. Rev. Lett. **121**, 147202 (2018).
[69] F. D. M. Haldane, Phys. Rev. Lett. **93**, 206602 (2004).
[70] K. Nomura, M. Koshino, and S. Ryu, Phys. Rev. Lett. **99**, 146806 (2007).
[71] T. Ando and T. Nakanishi, J. Phys. Soc. Jpn. **67**, 1704 (1998).
[72] Notice that in both cases the Landau level mixing effect is not considered, which may eventually destroy the CFL phase when the disorder strength exceeds the gap between different Landau levels.
[73] L. Amico, R. Fazio, A. Osterloh, and V. Vedral, Rev. Mod. Phys. **80**, 517 (2008).
[74] J. Eisert, M. Cramer, and M. B. Plenio, Rev. Mod. Phys. **82**, 277 (2010).
[75] N. Laflorencie, Phys. Rep. **646**, 1 (2016).
[76] M. Haque, O. Zozulya, and K. Schoutens, Phys. Rev. Lett. **98**, 060401 (2007).
[77] A.M Lauchli, E.J Bergholtz, and M. Haque, New J. Phys. **12**, 075004 (2010).
[78] Z. Liu and R. N. Bhatt, Phys. Rev. B **96**, 115111 (2017).
[79] Since the FQH phases host the degenerate states in the thermodynamic limit, we consider a ground state manifold containing the lowest six eigenstates to compute the density matrix ρ and related entanglement entropy. Please see the Supplemental Material [56].
[80] E. H. Rezayi, F. D. M. Haldane, and K. Yang, Phys. Rev. Lett. **83**, 1219 (1999).
[81] F. D. M. Haldane, E. H. Rezayi, and K. Yang, Phys. Rev. Lett. **85**, 5396 (2000).
[82] D. N. Sheng, Ziqiang Wang, and B. Friedman, Phys. Rev. B **66**, 161103(R) (2002).